25. Pryor, W. A., Church, D. F., Govinden, C. K. & Crank, G. *J. org. Chem.* **47,** 156–159 (1982).
26. Feelisch, M. *J. cardiovasc. Pharmac.* **17** (suppl. 3), S25–S33 (1991).
27. Sucher, N. J. & Lipton, S. A. *J. Neurosci. Res.* **30,** 582–591 (1991).
28. Choi, D. W. *Neuron* **1,** 623–634 (1988).
29. Meldrum, B. & Garthwaite, J. *Trends pharmacol. Sci.* **11,** 379–387 (1990).
30. Lipton, S. A. *Trends Neurosci.* **15,** 75–79 (1992).
31. Bredt, D. S., Hwang, P. M. & Snyder, S. H. *Nature* **347,** 768–770 (1990).
32. Liu, T. H., Beckman, J. S. Freeman, B. A., Hogan, E. L. & Hsu, C. Y. *Am. J. Physiol.* **256,** 589–593 (1989).
33. Kinouchi, H. *et al. Proc. natn. Acad. Sci. U.S.A.* **89,** 11158–11162 (1991).
34. Stamler, J. S. *et al. Proc. natn. Acad. Sci. U.S.A.* **89,** 444–448 (1991).

ACKNOWLEDGEMENTS. We thank J. S. Beckman and L. K. Keefer for helpful discussion, J. Hartman for an early set of experiments in this study, and M. E. Mullins for assistance in preparing the peroxynitrite. This work was supported by grants from the USPHS, American Foundation for AIDS Research (AmFAR), and American Heart Association. S.Z.L. is an AmFAR/ Pediatric AIDS Foundation Scholar. J.S.S. is a Pew Scholar in the Biomedical Sciences.

Control of cell fate in *C. elegans* by a GLP-1 peptide consisting primarily of ankyrin repeats

Henry Roehl & Judith Kimble

Departments of Genetics and Biochemistry and
Laboratory of Molecular Biology, University of Wisconsin-Madison,
Madison, Wisconsin 53706-1596, USA

THE homologous proteins GLP-1 and LIN-12 are required for cell interactions during nematode development[1–5]. *glp-1* and *lin-12* are members of a gene family that includes *Drosophila Notch* and several vertebrate homologues[6]. The members of this family have a single transmembrane domain and a similar arrangement of repeated amino-acid motifs (see Fig. 1). The mechanism by which proteins in this family function is not understood. One hypothesis is that these proteins are receptors, each with an extracellular domain that binds a ligand and an intracellular domain that influences the activity of downstream cell fate regulators. Here we report that a region of the GLP-1 intracellular domain, consisting primarily of six ankyrin repeats, is sufficient to direct cell fate. The cell fate transformations seen are similar to transformations caused by gain-of-function mutations in either *glp-1* or *lin-12* and do not rely on endogenous *lin-12* or *glp-1* activity. We propose that the ankyrin repeat region of GLP-1 is responsible for controlling downstream regulators of cell fate.

To investigate the mechanism by which GLP-1 regulates cell fate, we constructed a plasmid designed to express the ankyrin repeat region of GLP-1 under control of a heat shock promoter (Fig. 1*b*). The ankyrin repeat region includes the six ankyrin repeats (218 amino acids) plus flanking residues, but does not contain the transmembrane domain or PEST sequence from the carboxy terminus (Fig. 1*b* legend). The C-terminal flanking residues (33 amino acids) make up a degenerate ankyrin repeat[25], and the amino-terminal flanking residues (52 amino acids) do not contain a known motif. As a control, we made a plasmid with the equivalent insert from a loss-of-function mutant, *glp-1*(*q224*), which contains a missense mutation in the fourth ankyrin repeat[7]. Transgenic animals carrying either wild-type or mutant ankyrin constructs, called HS-ANK(+) or HS-ANK(−), respectively, express protein in a heat-shock-dependent manner (Fig. 1*c*).

Animals expressing the HS-ANK(+) transgene exhibit a number of somatic cell fate changes. The most obvious effect is the presence of multiple pseudovulvae, the Muv phenotype (Figs 2*a*, 3 and Table 1, see below). Both *glp-1* (ref. 9) and *lin-12* (ref. 3) gain-of-function (gf) mutants display a Muv phenotype. Other effects include transformation of the anchor cell to a ven-

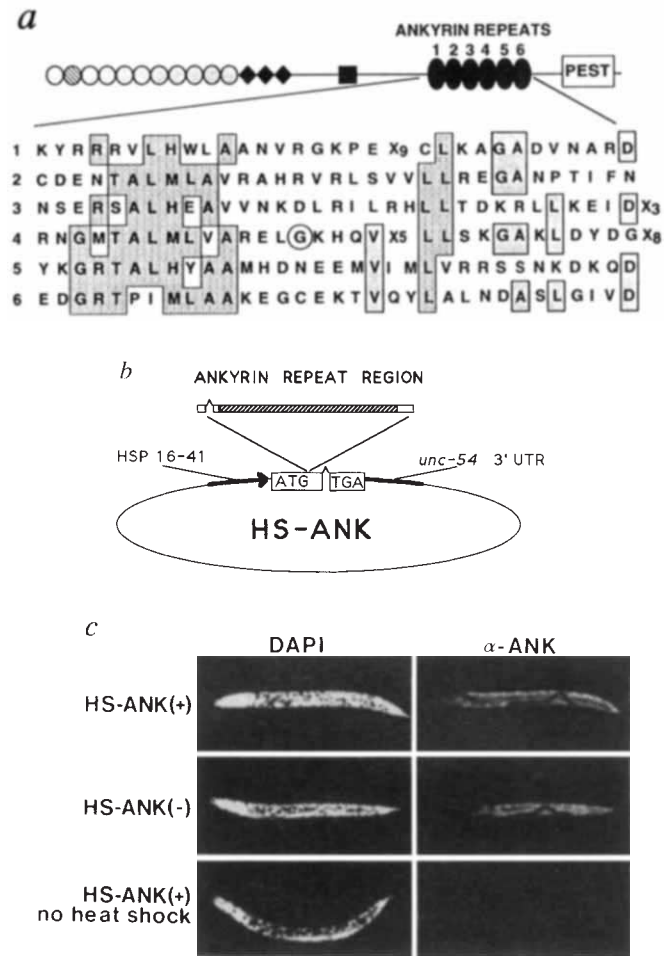

FIG. 1 Expression of the GLP-1 ankyrin repeat region in transgenic animals. *a*, The GLP-1 ankyrin repeats. Top, schematic of GLP-1. GLP-1 has 10 EGF-like repeats (grey circles), 3 LNG repeats (solid diamonds), a transmembrane domain (solid square), 6 ankyrin repeats (solid ovals), and a PEST sequence (see refs 5 and 7 for more detail). Bottom, the 6 ankyrin repeats, also known as *cdc10/sw16* repeats[26]. Shaded amino acids occur in at least 3/6 repeats. The circled glycine is changed to glutamic acid in *glp-1*(*q224*)[7]. *b*, HS-ANK plasmids. *c*, Protein expression of HS-ANK(+) and HS-ANK(−) transgenes. Animals were heat shocked at 33 °C for 1 h, allowed to recover at 20 °C, and stained with DAPI (left) or with polyclonal antibodies specific for the GLP-1 ANK repeat region (right). Top, HS-ANK(+) [*qIs1; dpy-4*] after 1 h heat shock. Middle, HS-ANK(−) [*qIs2 dpy-4*] after 1 h heat shock. Bottom, HS-ANK(+) [*qIs1; dpy-4*] with no heat shock. The HS-ANK protein is primarily cytoplasmic (data not shown). There was no difference between the level of expression or the protein stability between HS-ANK(+) and HS-ANK(−); after a 1-h period of recovery, staining was bright; after a 4-h period of recovery, staining was easily detectable (data not shown); and after an 8-h period of recovery, staining was faint (data not shown). Antibody methods will be reported elsewhere (S. Crittenden, E. Troemel and J.K., manuscript in preparation). Scale bar, 0.1 mm.
METHODS. Plasmids were constructed from pPD49.83 (provided by A. Fire), which contains heat-shock promoter HSP16-41[8]. The insert encodes the ankyrin repeats (cross-hatched), the seventh degenerate ankyrin repeat at the C terminus (SMDMTAAQVAEASYHHELAAFLRQVANERHRND; single-letter amino-acid code) and 52 amino acids at the N terminus (PGDYNELNFDFQSETFAPADLPADEIPLHVQAAGPDAITAPITNESVNQVDS). HS-ANK(+) is wild-type, whereas HS-ANK(−) carries the equivalent fragment from *glp-1*(*q224*). Transgenic lines were generated in wild-type hermaphrodite animals (var. Bristol) using *rol-6*(*su1006*) as a cotransformation marker[19]. 10/10 HS-ANK(+) lines and 0/10 HS-ANK(−) produced Muv animals after heat shock. Integrants were made with γ-irradiation (3,500 rads): *qIs1* carries HS-ANK(+) integrated on LG*I* and *qIs2* carries HS-ANK(−) on LG*IV*. *qIs1* and *qIs2* were placed into a *dpy-4*(*e1166*) homozygous background to suppress the *rol-6* cotransformation marker.

tral uterine precursor in the hermaphrodite somatic gonad and formation of multiple proximal hooks in male tails (Fig. 2*a* and legend). Both of these cell fate changes are typical of *lin-12(gf)* mutants[3]. No fate transformations were observed in HS-ANK(+) animals without heat shock or HS-ANK(−) animals after heat shock (Figs 2*b*, 3 and Table 1). Although the endogenous *glp-1(q224)* gene is temperature sensitive, no effect of HS-ANK(−) was observed when animals were maintained at permissive temperature (15 °C) after heat shock. We did not see effects in the germ line, where *glp-1* normally functions[1]. This is probably because expression from the heat-shock promoter is strongest in somatic tissues[8].

Here we focus on the effect of HS-ANK(+) in the vulval hypodermis, because effects of both GLP-1 and LIN-12 on this tissue have been documented in detail[3,9]. Normally, LIN-12 mediates cell–cell signalling within the vulval hypodermis so that two of the six vulval precursor cells follow the VH2 fate[3] (Fig. 3*b*). By contrast, gain-of-function mutations in both *glp-1* and *lin-12* cause all six vulval precursor cells to follow a VH2-like fate resulting in a Muv phenotype (Fig. 3*c*). Genetic and molecular data suggest that this Muv phenotype is the result of deregulation of GLP-1 or LIN-12, which leads to an increase of their activity in the vulval lineages[9,10].

To determine the effect of HS-ANK(+) on vulval cell fate, we first examined the dependence of the Muv phenotype on the anchor cell. In wild-type animals, vulval development is induced by the somatic gonadal anchor cell[11], but in mutants with deregulated LIN-12 or GLP-1 activity, the Muv phenotype is independent of anchor cell induction[3,9]. Although heat-shocked HS-ANK(+) animals have no apparent anchor cell (see above), we eliminated the entire gonad by laser ablation to ensure removal of all anchor cell activity. Such gonadless animals were nonetheless Muv after a heat shock in L2 lethargus (24/24 animals) (Fig. 2*c*). Therefore, the effect of HS-ANK(+) on vulval development is similar to that of deregulated LIN-12 and GLP-1 in its independence from the anchor cell.

We next investigated when HS-ANK(+) animals must be heat shocked to achieve the Muv phenotype. Deregulated GLP-1

TABLE 1 Characterization of HS-ANK(+)-induced Muv phenotype

(*a*) HS-ANK(+) is required during L2 or early L3 to generate multiple pseudovulvae

Transgene	Stage of heat shock	Number of pseudovulvae per animal 0	2	3	4	5	6
HS-ANK(+)	Hatch	>20	0	0	0	0	0
HS-ANK(+)	Mid-L1	>20	0	0	0	0	0
HS-ANK(+)	L1 lethargus	21	6	6	3	0	0
HS-ANK(+)	Mid-L2	3	3	10	10	5	1
HS-ANK(+)	L2 lethargus	0	2	6	20	14	2
HS-ANK(+)	Mid-L3	19	5	7	4	0	0
HS-ANK(+)	L3 lethargus	>20	0	0	0	0	0
HS-ANK(+)	Mid-L4	>20	0	0	0	0	0
HS-ANK(−)	Hatch	>20	0	0	0	0	0
HS-ANK(−)	Mid-L1	>20	0	0	0	0	0
HS-ANK(−)	L1 lethargus	>20	0	0	0	0	0
HS-ANK(−)	Mid-L2	>20	0	0	0	0	0
HS-ANK(−)	L2 lethargus	>20	0	0	0	0	0
HS-ANK(−)	Mid-L3	>20	0	0	0	0	0
HS-ANK(−)	L3 lethargus	>20	0	0	0	0	0
HS-ANK(−)	Mid-L4	>20	0	0	0	0	0

(*b*) HS-ANK(+) does not depend on endogenous LIN-12 or GLP-1 to regulate vulval fate

Transgene	Genotype	Number of pseudovulvae per animal 0	2	3	4	5	6
HS-ANK(+)	Wild-type	0	0	12	9	3	0
HS-ANK(+)	*lin-12(n137e2032)*	0	2	6	20	14	2
HS-ANK(+)	*lin-12(n137n720)*	0	4	7	8	1	0
HS-ANK(+)	*lin-12(n941)*	0	1	1	12	1	0
HS-ANK(+)	*glp-1(q175)*	0	2	4	7	3	0

a, Staged animals carrying highly penetrant extrachromosomal arrays (*qEx58*, HS-ANK(+) or *qEx59*, HS-ANK(−)) were heat shocked at 33 °C for 1 h, and the number of pseudovulvae per animal was determined in either L4s or young adults using Nomarski microscopy. Animals with 0 pseudovulvae had one vulva. Larval stages are designated L1–L4 for first through fourth larval stages. To obtain animals at hatching or in lethargus, worms were identified by size and pharyngeal activity. To obtain animals in mid-L1, newly hatched larvae were incubated for 9 h; to obtain animals in mid-L2, mid-L3, or mid-L4, larvae in L1, L2, or L3 lethargus, respectively, were incubated for 5 h. *b*, Animals homozygous for an integrated copy of HS-ANK(+) (*qIs1; dpy-4*) or HS-ANK(−) (*qIs1 dpy-4*) and also homozygous for mutations in either *lin-12* or *glp-1* were heat shocked in L2 lethargus for 1 h at 33 °C. Two *lin-12* mutants carry both a gain-of-function (*n137*) and a loss-of-function mutation in *cis*[3]; the single mutant, *lin-12(n941)*, has a severe loss-of-function phenotype[3]; *glp-1(q175)* is a null allele and carries a nonsense mutation mapping within the EGF-like repeats[1,7].

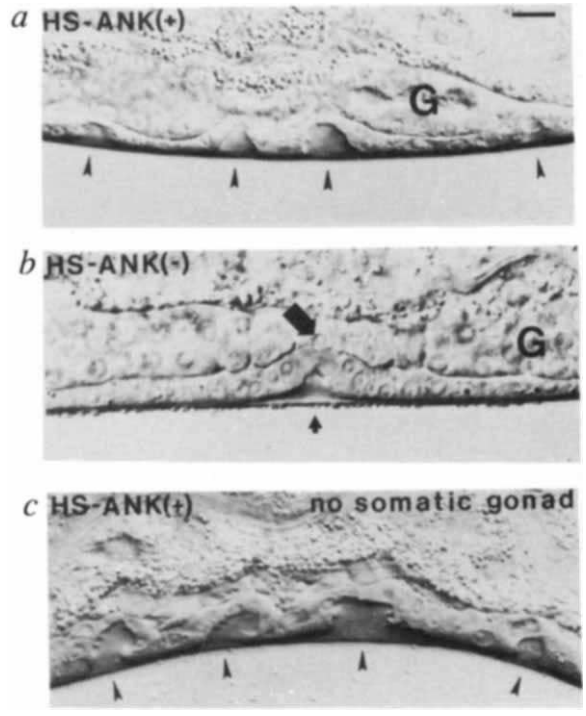

FIG. 2 Expression of HS-ANK(+) generates multiple pseudovulvae. Left, Nomarski differential interference contrast (DIC) photomicrographs of fourth larval stage (L4) hermaphrodites. Scale bar, 0.01 mm. *a*, HS-ANK(+) [*qIs1; dpy-4*]. Four pseudovulvae are present (arrowheads); G, somatic gonad. Note that an anchor cell is not present; the anchor cell was absent in 21/21 animals. In addition, in XO males, 7/9 HS-ANK(+) animals had two proximal hooks after heat shock, a fate transformation in the male hypodermis that is analogous to production of multiple pseudovulvae in hermaphrodites. *b*, HS-ANK(−) [*qIs2 dpy-4*]. A normal vulva is formed (arrow) and an anchor cell is present (large arrow) in the somatic gonad; G, somatic gonad. *c*, HS-ANK(+) [*qIs1; dpy-4*] animal in which the somatic gonad was eliminated by later ablation. Four pseudovulvae are made; no gonad is present.
METHODS. Animals were heat shocked at 33 °C for 1 h during L2 lethargus, which just precedes the moult to L3. The gonadless animal in *c* was obtained by eliminating the two precursor cells of the somatic gonad, Z1 and Z4, by laser ablation in early L1. Laser microsurgery was done as described[20] using a VSL-337 nitrogen laser and DLM-110 dye laser module. All animals in this paper were maintained at 20 °C using standard laboratory procedures[21] unless noted otherwise.

and LIN-12 act during late L2 or early L3 for this phenotype[3,9]. Similarly, HS-ANK(+) must be expressed during late L2 or early L3 to achieve the strongest Muv effect: the most Muv animals and the most pseudovulvae per animal occurred after heat shocks during L2 lethargus (Fig. 3*a*, Table 1*a*).

Finally we examined lineages of the vulval precursor cells after heat shock. Again, we found that HS-ANK(+) has an effect that is remarkably similar to that of deregulated GLP-1 or LIN-12. Specifically, expression of HS-ANK(+) transformed all six vulval precursor cells (VPCs) to a VH2 or a VH2-like fate (Fig. 3*c*). As expected, this lineage transformation is independent of the anchor cell, but is dependent on the presence of the HS-ANK(+) transgene (Fig. 3*c*). Therefore, by three criteria (anchor cell independence, temporal requirement and lineage) the HS-ANK(+) transgene mimics the effect of deregulated GLP-1 or LIN-12 on vulval development.

The ankyrin repeat region encoded by HS-ANK(+) might act independently or it might activate endogenous GLP-1 or LIN-12. To distinguish between these possibilities, we examined the effect of HS-ANK(+) in three *lin-12* loss-of-function mutants and one *glp-1* null mutant. HS-ANK(+) induces a Muv phenotype despite the lack of endogenous GLP-1 or LIN-12 (Table 1*b*). We cannot test the effect of HS-ANK(+) in the absence of both GLP-1 and LIN-12, because the double mutant

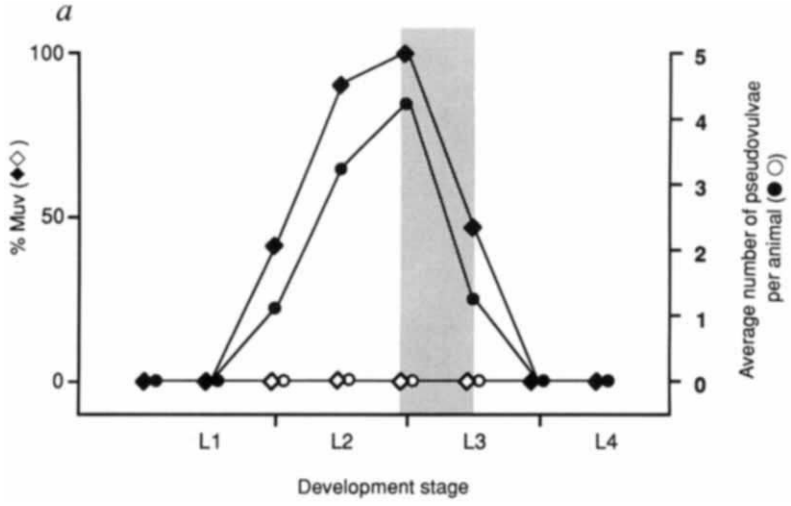

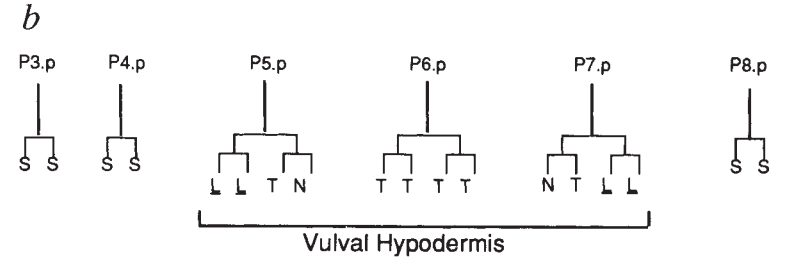

c

Genotype	Gonad	P3.p	P4.p	P5.p	P6.p	P7.p	P8.p
HS-ANK(+)	+	LLLT	LLTN	LLTN	TNNT	NTLL	NLLL
HS-ANK(+)	+	LLTL	LLTL	LLTN	NTLL	NTLL	LLLL
HS-ANK(+)	-	NLLL	LLLL	LLTN	LNDD	LLLL	LLNL
HS-ANK(+)	-	NONL	LLTN	LLTN	LLLN	LLLN	LLLN
HS-ANK(-)	+	SS	SS	LLTN	TTTT	NTLL	SS
glp-1(gf)	-	S LL	SS	SNLL	LLNN	LLLL	SS
	-	SS	LLS	LTLL	LLLT	LLLN	LL S
lin-12(gf)	+	SS	SS	LLLN	LLLL	NTLL	LLLL

FIG. 3 *a*, HS-ANK(+) expression is required at the time of VPC determination. Percentage of animals with multiple vulvae and average number of pseudovulvae per animal are plotted against the stage of development at which heat shock was delivered. Averages draw from data details in Table 1. The developmental stage at which heat shock of HS-ANK(+) is most effective in generating pseudovulvae coincides remarkably well with the developmental stage at which the VPC cells are determined[11] and at which *lin-12(gf)* and *glp-1(gf)* control vulval fates[3,9]. (shaded region). Open symbols, HS-ANK(−); closed symbols, HS-ANK(+). *b*, *c*, HS-ANK(+) transformation of vulval precursor cell (VPC) lineages. The following conventions[22] are used to describe cell divisions: L, longitudinal axis of division; T, transverse axis of division; N, no division; O, oblique division; D, division; underline indicates that daughters adhere to the cuticle; S, syncytial hypodermis. In addition, we use a dashed underline to indicate adherence to the cuticle for at least 4 h after the division. *b*, Wild-type VPC lineages. Three of six VPCs, P5.p, P6.p and P7.p, generate a total of 22 descendants to form the vulval hypodermis (see ref. 23 for review). Normally, P6.p produces 8 cells by a series of four transverse divisions, a fate called VH1 or 1°, and P5.p and P7.p each produces 7 cells by a series of terminal divisions described as *LL*TN (NT*LL* is the same pattern with reversed symmetry), a fate called VH2 or 2°. Normally, the VH1 and VH2 fates are dependent on induction by the somatic gonadal anchor cell[11], and the choice between VH1 and VH2 fates is dependent on lateral signalling among the VPCs[20], which is mediated by LIN-12[3]. The three other VPCs, P3.p, P4.p and P8.p, divide once and fuse with the hypodermal syncytium. *c*, The effect of HS-ANK(+) on the VPC lineages mimics that of unregulated LIN-12 or GLP-1. In *glp-1(gf)* or *lin-12(gf)* mutants all six VPCs adopt a VH2 or VH-like fate[3,9]. Similarly, in HS-ANK(+) transgenic animals, all six VPCs, P3–8.p, follow a pattern of division similar to that of the VH2 or 2° fate. As in the VPC lineages of *glp-1(gf)* and *lin-12(gf)* mutants, lineages of the HS-ANK(+) VPCs vary from animal to animal and do not always follow the precise *LL*TN pattern of division that defines VH2. Nonetheless, divisions of P3–8.p in HS-ANK(+) exhibit the hallmark features of VH2, which are longitudinal (L) rather than transverse (T) divisions and adherence to the cuticle. In marked contrast to the VH2/VH2-like fates observed in wild-type animals or *glp-1(gf)* or *lin-12(gf)* mutants, all cells in HS-ANK(+) remained adherent to the cuticle 4–6 h after the terminal division. We show this feature in the figure by using a dashed underline as described above. Some of the cells must eventually become non-adherent to allow the formation of the pseudovulvae. We did not observe which cells did this, so all of the VPCs are underlined with dashes. This extreme adherence exaggerates a feature typical of VH2 and may therefore reflect stronger activity in the case of HS-ANK(+) than has been reported previously for either deregulated GLP-1 or LIN-12[3,9].

METHODS. HS-ANK(+), [*qIs1; dpy-4*]; HS-ANK(−), [*qIs2 dpy-4*]. Lineages were obtained by examination of cell divisions as previously described[24]. Gonadless animals were obtained as described in the legend to Fig. 2. The *glp-1(gf)* and *lin-12(gf)* lineages are from ref. 9.

dies before vulva development has begun[12]. But wild-type GLP-1 is not detectable in the vulva with antibodies (S. Crittenden, personal communication) and loss of GLP-1 has no phenotypic effect on the vulva[1]. Therefore, no functional LIN-12 or GLP-1 is likely to be present in the vulval lineages of the *lin-12(lf)* mutants. The simplest explanation is that the ankyrin repeat region is sufficient to regulate cell fate.

Our findings support two major conclusions. First, the ankyrin repeat region is the active part of the protein for controlling cell fate. This conclusion eliminates the model that the primary role of GLP-1 is adhesion[13] and supports the model that its primary role is signal transduction[4,5]. Second, because the ankyrin repeat region is active when separated from the rest of the protein, the function of other regions of GLP-1 (for example the extracellular domain) may be to modulate the activity of the ankyrin repeat region.

How might the ankyrin repeat region of GLP-1 regulate cell fate? All six of the intracellular missense mutations of *glp-1* are loss-of-function and map to the ankyrin repeats[7]. Based on the site of these mutations, we proposed that the ankyrin repeats are essential to GLP-1 function. The molecular analysis of mutations, together with the results presented here, suggest that the ankyrin repeats themselves are responsible for the transgene activity. In addition, the amino acids flanking the ankyrin repeats, which are also encoded by the HS-ANK transgene, may contribute to its activity.

It is intriguing that ankyrin repeats of other regulatory proteins are essential to their function[14]. For example, the ankyrin repeats of $I_\kappa B$ bind $NF_\kappa B$ and prevent entry into the nucleus[15], and the ankyrin repeats of the β-subunit of GABP bind the α-subunit to allow DNA binding of the heterodimer[16]. We speculate that the GLP-1 ankyrin repeats bind a downstream target protein and influence the activity of that protein to control cell fate. The ankyrin repeat region of GLP-1 may represent a new type of active domain for receptors. Unlike an enzymatic activity, such as a tyrosine kinase, GLP-1 functions through the ankyrin repeat region and perhaps through protein–protein interactions. Furthermore, we speculate that the equivalent region may be critical to the function of similar proteins, such as Notch and vertebrate homologues (such as *int-3*[17] and TAN-1[18]). □

Received 1 June; accepted 21 July 1993.

1. Austin, J. & Kimble, J. *Cell* **51,** 589–599 (1987).
2. Priess, J. R., Schnabel, H. & Schnabel, R. *Cell* **51,** 610–611 (1987).
3. Greenwald, I. S., Sternberg, P. W. & Horvitz, H. R. *Cell* **34,** 435–444 (1983).
4. Austin, J. & Kimble, J. *Cell* **58,** 565–571 (1989).
5. Yochem, J. & Greenwald, I. *Cell* **58.** 553–563 (1989).
6. Artavanis-Tsakonas, S., Delidakis, C. & Fehon, R. G. *A. Rev. Cell Biol.* **7,** 427–452 (1991).
7. Kodoyianni, V., Maine, E. M. & Kimble, J. *Molec. Biol. Cell* **3,** 1199–1213 (1992).
8. Stringham, E. G., Dixon, D. K., Jones, D. & Candido, E. P. M. *Molec. Biol. Cell* **3,** 221–233 (1992).
9. Mango, S. E., Maine, E. M. & Kimble, J. *Nature* **352,** 811–815 (1991).
10. Greenwald, I. & Seydoux, G. *Nature* **346,** 197–199 (1990).
11. Kimble, J. *Devl Biol.* **87,** 286–300 (1981).
12. Lambie, E. J. & Kimble, J. *Development* **112,** 231–240 (1991).
13. Greenspan, R. J. *New Biol.* **2,** 595–600 (1990).
14. Nolan, G. P. & Baltimore, D. *Curr. Opin. Genet. Dev.* **2,** 211–220 (1992).
15. Beg, A. A. *et al. Genes Dev.* **6,** 1899–1913 (1992).
16. Thompson, C. C., Brown, T. A. & McKnight, S. L. *Nature* **253,** 762–768 (1991).
17. Robbins, J., Blondel, B. J., Gallahan, D. & Callahan, R. *J. Virol.* **66,** 2594–2599 (1992).
18. Ellisen, L. W. *et al. Cell* **66,** 649–661 (1991).
19. Mello, C. C., Kramer, J. M., Stinchcomb, D. & Ambros V. *EMBO J.* **10,** 3959–3970 (1991).
20. Sulston, J. E. & White, J. G. *Devl Biol.* **78,** 577–597 (1980).
21. Brenner, S. *Genetics* **77,** 71–94 (1974).
22. Ferguson, E. L., Sternberg, P. W. & Horvitz, H. R. *Nature* **326,** 259–267 (1987).
23. Horvitz, H. R. & Sternberg, P. W. *Nature* **351,** 535–541 (1991).
24. Sulston, J. & Horvitz, H. R. *Devl Biol.* **56,** 110–156 (1977).
25. Lissemore, J. & Maine, E. *Genetics* (in the press).
26. Breeden, L. & Nasmyth, K. *Nature* **329,** 651–654 (1987).

ACKNOWLEDGEMENTS. We thank S. Crittenden for the antibodies and assistance with their use and interpretation, A. Fire for pPD49.83 and discussion about plasmid design, members of the laboratory for discussion and critical comments on the manuscript and L. Olds for technical assistance. Some strains used in this work were provided by the *Caenorhabditis* Genetics Center, which is funded by the NIH.

Mechanism of presynaptic inhibition by neuropeptide Y at sympathetic nerve terminals

Peter T. Toth, Vytautas P. Bindokas, David Bleakman*, William F. Colmers† & Richard J. Miller‡

Department of Pharmacological and Physiological Sciences, University of Chicago, 947 East 58th Street, Chicago, Illinois 60637, USA
† Department of Pharmacology, University of Alberta, Edmonton, Alberta T6G 2H7, Canada

CALCIUM influx through voltage-sensitive Ca^{2+} channels is the normal physiological stimulus for the activity-dependent release of neurotransmitters at synaptic contacts. It has been postulated that presynaptic inhibition of transmitter release is due to a reduction in Ca^{2+} influx at the nerve terminal, which could result from the direct inhibition of Ca^{2+} channels. Neuropeptide Y and noradrenaline act as cotransmitters at many sympathetic synapses. Both of these substances produce presynaptic inhibition and can inhibit Ca^{2+} currents in the soma of sympathetic neurons[1–5]. Here we provide direct evidence that presynaptic inhibition produced by neuropeptide Y at sympathetic nerve terminals is associated with a reduction in Ca^{2+} influx and that this is due to the selective inhibition of neuronal N-type Ca^{2+} channels.

We examined the effects of neuropeptide Y (NPY) on Ca^{2+} signals in single nerve terminals of sympathetic neurons from rat superior cervical ganglia that were co-cultured with atrial myocytes. Co-cultures consisted of clearly identified sympathetic neurons which extended axons to a myocyte (for example, see Figs 1*B*, 2*A*). As described previously, in low-density co-cultures of sympathetic neurons and cardiac myocytes, the neurons possess varicosities that contain transmitter[6] and form functional synapses with the myocytes[7]. To find out whether functional synaptic contacts existed in our co-cultures, we recorded spontaneous oscillations in the intracellular free Ca^{2+} concentration ($[Ca^{2+}]_i$) of the atrial myocytes while evoking action potentials in presynaptic neurons using a patch electrode. Stimulation of the sympathetic neuron produced changes in the frequency of these spontaneous Ca^{2+} oscillations and in the associated contraction frequency of the coupled myocyte, indicating that functional synaptic contacts existed between the two cells (Fig. 1*A*). The effect of neuronal stimulation on myocyte activity could be inhibited by a combination of adrenergic and cholinergic blockers[8,9]. As shown in Fig. 1*A*, *b*, NPY (300 nM) produced no effect on the spontaneous contractions of the myocytes, but prevented the evoked reduction in myocyte activity. Thus NPY produced presynaptic inhibition in these cultures, as it does in isolated preparations of sympathetic neuroeffector junctions[10,11].

Synaptic areas were visualized using the fluorescent styryl dye RH414, which becomes trapped in synaptic vesicles during exo- and endocytosis, thus staining active terminals in a use-dependent manner (Fig. 1*C*)[12]. Terminals labelled in this way appeared as areas of punctate fluorescence overlaying target myocytes. Neurons were also filled with Fura-2 using patch electrodes (Fig. 1*D*). The $[Ca^{2+}]_i$ in terminals could now be measured by selectively imaging areas of combined Fura-2 and RH414 fluorescence ('synaptic areas'). When neurons were stimulated to fire trains of 40 action potentials, areas corresponding to terminal

* Present address: Lilly Research Centre, Erl Wood Manor, Windlesham, Surrey GU2 0PH, UK.
‡ To whom correspondence should be addressed.